Journal of Ceramic Processing Research. Vol. 17, No. 4, pp. 322~326 (2016)

J O U R N A L O F
Ceramic Processing Research

Properties and rapid consolidation of nanostructured WC and WC-10 vol.%$TiAl_3$ hard materials by the high frequency induction heating

Dong-Gu Lee[a], Jin-Kook Yoon[b] and In-Jin Shon[a,*]

[a]*Division of Advanced Materials Engineering and the Research Center of Advanced Materials Development, Engineering College, Chonbuk National University, Chonbuk 561-756, Korea*

[b]*Materials Architecturing Research Center, Korea Institute of Science and Technology, PO Box 131, Cheongryang, Seoul 130-650, Korea*

In the case of cemented WC, Ni or Co is added as a binder for the formation of composite structures. However, the high cost and the low hardness of Ni or Co, and the low corrosion resistance of the WC-Ni and WC-Co cermets have generated interest in recent years for alternative binder phases. In this study, $TiAl_3$ was used as a novel binder and consolidated by the high frequency induction heated sintering (HFIHS) method. The method was found to enable not only the rapid densification but also the inhibition of grain growth preserving the nano-scale microstructure. Highly dense WC and WC-$TiAl_3$ with a relative density of up to 99% was obtained within one min by HFIHS under a pressure of 80 MPa. The addition of $TiAl_3$ to WC enhanced the toughness without great decrease of hardness due to crack deflection and nanostructured phase.

Key words: Nanomaterials, Sintering, Hardness, Fracture Toughness, Powder Metallurgy.

Introduction

The attractive properties of WC are high hardness and relatively high thermal and electrical conductivities. WC has also high chemical stability, with melting temperatures of 3058 K, and they do not undergo phase transformations. It is used extensively in cutting tool and abrasive materials in composite with a binder metal, such as Co or Ni. The binder phase has inferior chemical characteristics compared to the carbide phase. Most notably, corrosion and oxidation occur preferentially in the binder phase [1]. Hence, the high cost and the low hardness of Ni or Co and the low corrosion resistance of the WC-Ni or WC-Co cermet have generated interest in recent years to find alternative binder phases [2, 3]. It has been reported that FeAl shows a higher oxidation resistance, a higher hardness and a cheaper materials compared to Ni or Co [4].

The improvement of mechanical properties and stability of cemented carbides could be achieved through microstructural changes such as grain size refinement [5, 6]. Nanocrystalline materials possess a high strength and hardness as well as excellent ductility and toughness, they have garnered more attention recently [7, 8]. Recently, nanocrystalline powders have been produced by high-energy milling [9, 10]. The sintering temperature of high-energy mechanically milled powder is lower than that of unmilled powder due to the increased reactivity, internal and surface energies, and surface area of the milled powder, which contribute to its so-called mechanical activation [11-13]. However, the grain size in sintered materials becomes much larger than that in pre-sintered powders due to fast grain growth during conventional sintering. Therefore, even though the initial particle size of (W,Ti)C is less than 100 nm, the grain size increases rapidly up to 2 μm or larger during conventional sintering [14]. Controlling grain growth during sintering is one of the keys to the commercial success of nanostructured materials. In this regard, the high frequency induction heated sintering method (HFIHS), which can make dense materials within 2 minutes, has been shown to be effective in achieving this goal [15-18].

We present here the results of the sintering of WC and WC-$TiAl_3$ composites by a high frequency induction heated sintering with simultaneous application of induced current and high-pressure. The goal of this study was to produce dense and nanocrystalline WC and WC-$TiAl_3$ hard materials in very short sintering times (< 1 min). The effect of novel $TiAl_3$ binder on the mechanical properties (hardness and fracture toughness), sintering behavior and relative density of WC-$TiAl_3$ composites was also examined.

Experimental Procedures

The WC powder used in this research was supplied by Taegu Tec Co. The average particle size was about 0.5 μm and the purity was 99.8%. $TiAl_3$ (< 45 μm, 99% pure, Sejong Co.) was used as binder material. Powders of two compositions corresponding to WC, and WC-10 vol.%$TiAl_3$ were prepared by weighing and milled

*Corresponding author:
Tel : +82 63 270 2381
Fax: +82 63 270 2386
E-mail: ijshon@chonbuk.ac.kr

in a high-energy ball mill (Pulverisette-5 planetary mill) at 250 rpm for 10 hrs. WC-Co balls (9 mm in diameter) were used in a sealed cylindrical stainless steel vial under an argon atmosphere. The weight ratio of balls-to-powder was 30 : 1. The grain size of the powders was calculated from the full width at half-maximum (FWHM) of the diffraction peak by Suryanarayana and Grant Norton's formula [19].

$$B_r\,(B_{crystalline} + B_{strain})\cos\theta = k\,l / L + \eta\sin\theta \qquad (1)$$

where B_r is the full width at half-maximum (FWHM) of the diffraction peak after instrumental correction; $B_{crystalline}$ and B_{strain} are FWHM caused by small grain size and internal stress, respectively; k is constant (with a value of 0.9); λ is wavelength of the X-ray radiation; L and η are grain size and internal strain, respectively; and θ is the Bragg angle. The parameters B and B_r follow Cauchy's form with the relationship: $B = B_r + B_s$, where B and B_s are the FWHM of the broadened Bragg peaks and the standard sample's Bragg peaks, respectively.

The milled powders were placed in a graphite die (outside diameter, 35 mm; inside diameter, 10 mm; height, 40 mm) and then introduced into the high frequency induction heated sintering (HFIHS) system made by Eltek Co. in the Republic of Korea. A schematic diagram of this system is shown in Ref. [15-18]. The HFIHS apparatus includes a 15 kW power supply and a uniaxial press with a maximum load of 50 kN. The system was first evacuated and a uniaxial pressure of 80 MPa was applied. An induced current was then activated and maintained until the densification rate became negligible, as indicated by the observed shrinkage of the sample. Sample shrinkage was measured in real time by a linear gauge measuring the vertical displacement. Temperature was measured by a pyrometer focused on the surface of the graphite die. The heating rates were approximately 1600 K $minute^{-1}$ during the process. At the end of the process, the current was turned off and the sample was allowed to cool to room temperature. The process was carried out under a vacuum of 5.33 Pa.

The relative density of the sintered sample was measured by the Archimedes method. Microstructural information was obtained from product samples, which had been polished and etched using Murakami's reagent (10 g potassium ferricyanide, 10 g NaOH, and 100 ml water) for 1-2 minutes at room temperature. Compositional and microstructural analyses of the products were made through X-ray diffraction (XRD), scanning electron microscopy (SEM) with energy dispersive X-ray spectroscopy (EDS) and a field emission scanning electron microscope (FE-SEM). Vickers hardness was measured by performing indentations at a load of 20 kg_f and a dwell time of 15 s.

Results and Discussion

Fig. 1 shows FE-SEM images of WC, and WC-10 vol.%$TiAl_3$ powders milled for 10 h. The powders are very fine and have a round shape. X-ray diffraction patterns of the WC, and WC-10 vol.%$TiAl_3$ powders after milling for 10 h are shown in Fig. 2. The broadening of WC peaks due to crystallite refinement and strain is evident after milling for 10 hrs. The milling process is known to introduce impurities from the ball and/or container. However, in this study, peaks other than WC were not identified. Particle size of WC was calculated from the plot of $B_r\,(B_{crystalline} + B_{strain})\cos\theta$ versus sinθ in Suryanarayana and Grant Norton's formula [19] in Fig. 3. The average grain sizes of the WC in the WC, and WC-10 vol.%$TiAl_3$ powders after milling for 10 hrs calculated from the XRD data were about 21 and 18 nm, respectively.

The shrinkage displacement-time (temperature) curve provides an important information on the consolidation behavior. The shrinkage record of WC, and WC-10 vol.%$TiAl_3$ compacts under the applied pressure of 80 MPa is shown in Fig. 4. In all cases, as induced current was applied, thermal expansion shows in the range 1000 and 1200 °C according to $TiAl_3$ content. And then shrinkage displacement abruptly increased above the temperature. The application of the induced current resulted in shrinkage due to consolidation. The temperature of rapid shrinkage initiation was seen to reduce by the addition of $TiAl_3$. It is considered that it is related to the melting of $TiAl_3$ phase due to large

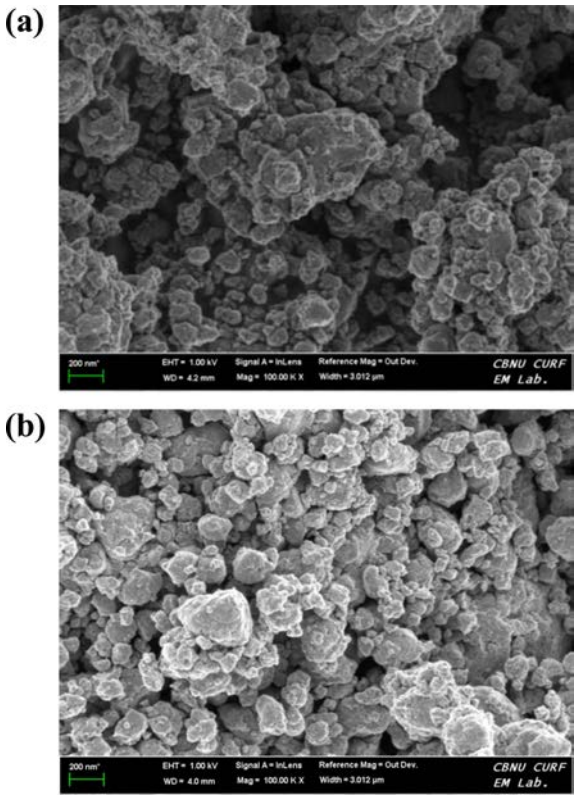

Fig. 1. FE-SEM images of the (a) WC, (b) WC-10vol.%$TiAl_3$ powders milled by high energy ball milling for 10hrs.

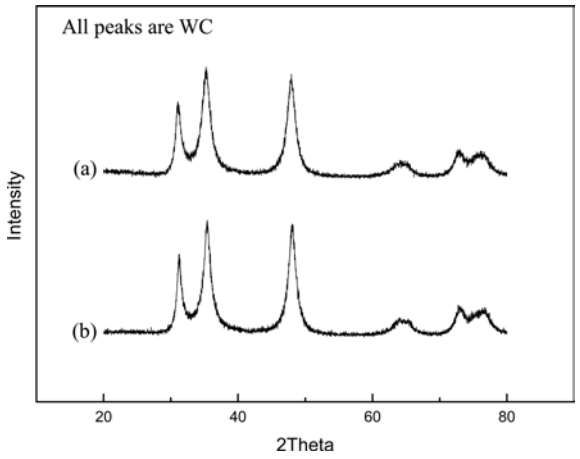

Fig. 2. X-ray diffraction patterns of the (a) WC, (b) WC-10 vol.%$TiAl_3$ powders milled by high energy ball milling for 10 hrs.

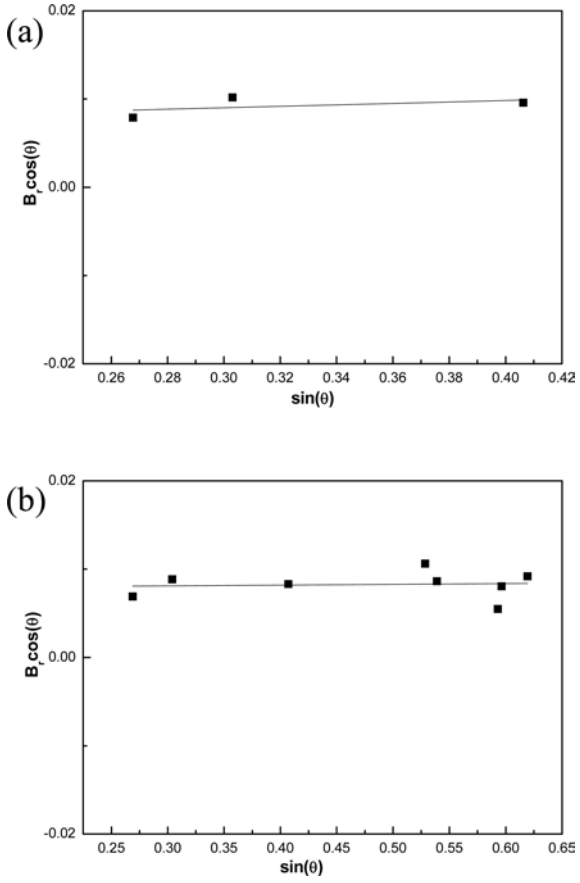

Fig. 3. Plots of B_r ($B_{crystallite} + B_{strain}$) cosθ versus sinθ for WC in (a) WC, and (b) WC-10 vol.%$TiAl_3$ powders after milling for 10 hrs.

Joule heat at contact of powders. Therefore, the main densification mechanism could be the rearrangement of carbide particles, enhancement of the diffusion, and viscous flow of the binder [20].

Fig. 5 shows the XRD patterns of WC, and WC-10 vol.%$TiAl_3$ after sintering. In all cases, only WC peaks are detected. The milling process is known to introduce impurities from the ball and/or container.

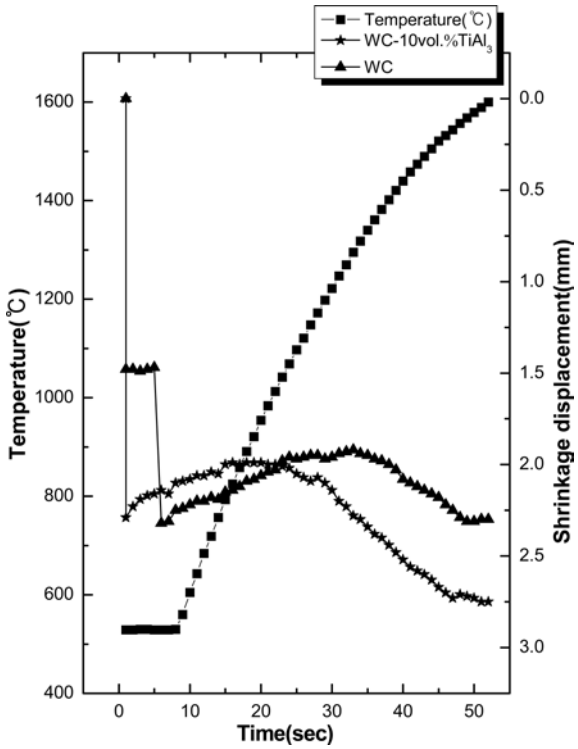

Fig. 4. Variations of temperature and shrinkage displacement with heating time during the sintering of WC and WC-10 vol.%$TiAl_3$ hard materials by HFIHS.

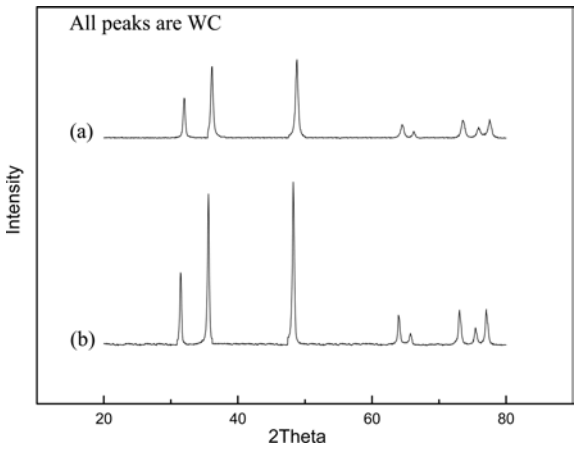

Fig. 5. XRD patterns of (a) WC, (b) WC-10vol.%$TiAl_3$ hard materials produced by HFIHS.

However, in this study, peaks other than WC were not identified. The average grain sizes of the WC calculated from the XRD data using Suryanarayana and Grant Norton's formula in Fig. 6 are about 121 and 77 nm for the samples with WC, and WC-10vol.%$TiAl_3$. FE-SEM images of the samples after being sintered up to about 1600 ºC are shown in Fig. 7. It is apparent that the WC grains consist of nanocrystallites suggesting the absence of grain growth during sintering. This retention of the fine grain structure can be attributed to the high heating rate and the relatively short exposure to the high temperature. Relative densities corresponding to WC,

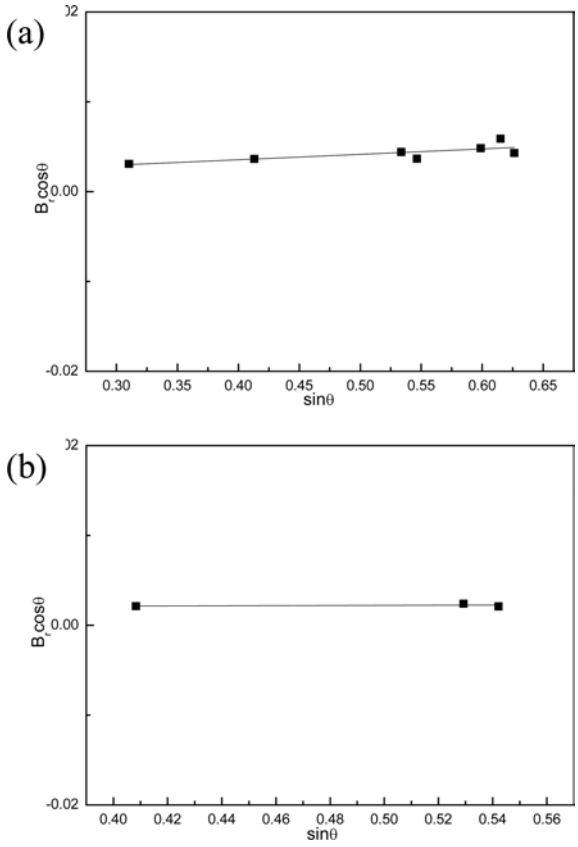

Fig. 6. Plots of B_r ($B_{crystallite} + B_{strain}$) cosθ versus sinθ for WC in (a) WC, and (b) WC-10 vol.%TiAl$_3$ sintered from powders after milling for 10 hrs.

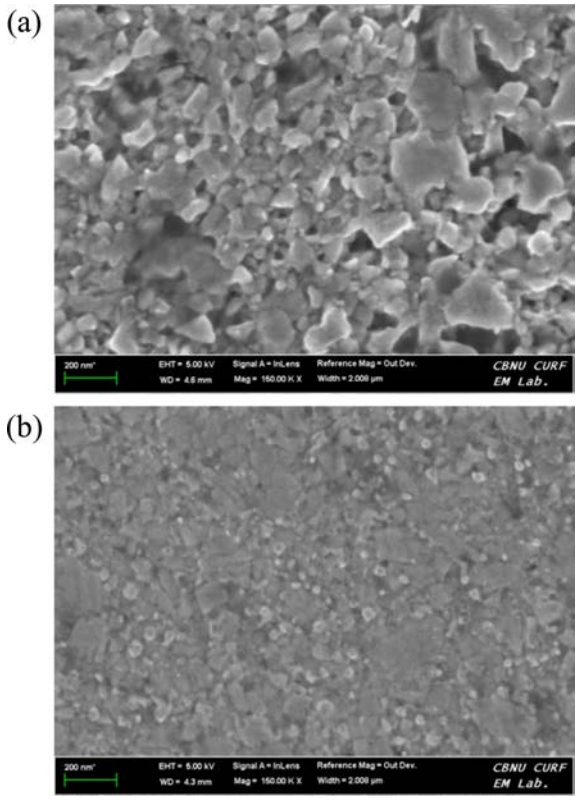

Fig. 7. FE-SEM images of (a) WC, (b) WC-10 vol.%TiAl$_3$ hard materials produced by HFIHS.

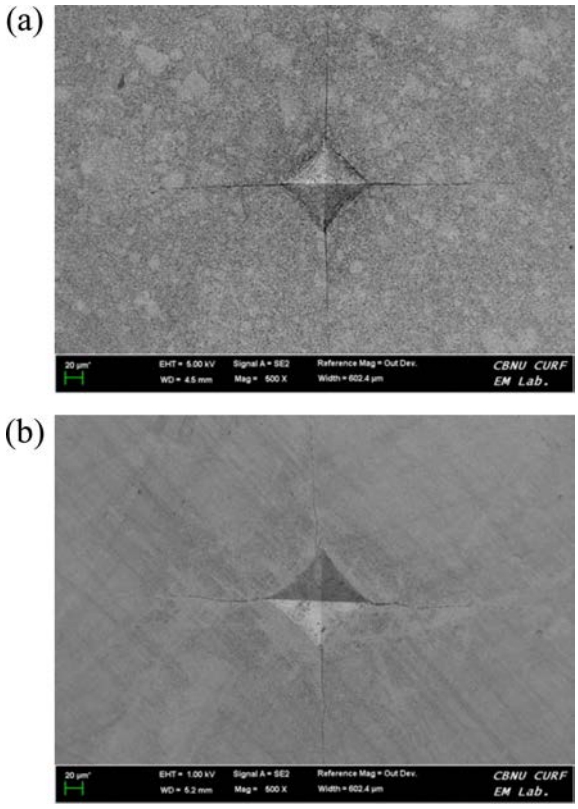

Fig. 8. Vickers hardness indentation of (a) WC, (b) WC-10vol.%TiAl$_3$ sintered by HFIHS.

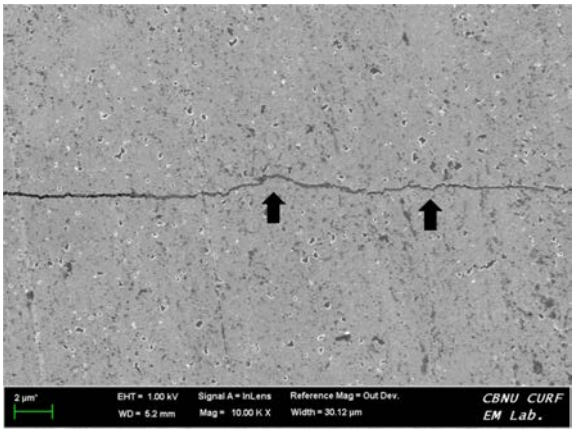

Fig. 9. Crack propagation in WC-10 vol.%TiAl$_3$ hard materials produced by HFIHS.

and WC-10 vol.%TiAl$_3$ were approximately 99 and 99.5%, respectively.

Vickers hardness measurements were performed on polished sections of the WC, and WC-10 vol.%TiAl$_3$ samples using a 20 kg$_f$ load and 15 s dwell time. Indentions with 20 kg$_f$ load produced median cracks around the indentation from which fracture toughness can be calculated. The lengths of these cracks permit estimation of the fracture toughness of the materials by means of the expression [21]:

$$K_{IC} = 0.203(c / a)^{-3/2} \cdot H_v \cdot a^{1/2} \quad (2)$$

where c is the trace length of the crack measured from the center of the indentation, a is one half of the average length of the two indent diagonals, and H_v is the hardness.

The Vickers hardness and the fracture toughness values of the WC, and WC-10 vol.%$TiAl_3$ samples were 2800 kg/mm^2, 6.2 MPa · m$^{1/2}$, and 2670 kg/mm^2, 9.5 MPa · m$^{1/2}$, respectively. These values represent the average of five measurements. The fracture toughness of WC-10 vol.%$TiAl_3$ samples is higher than that of monolithic WC without great decrease of hardness. The sintering method in this study was proven to be very effective to consolidate WC-$TiAl_3$ cermets. The hardness of metal carbide greatly decreased by addition of Co or Ni [22]. The use of $TiAl_3$ binder instead of Co or Ni is very effective especially to maintain the high hardness of monolithic WC without the expense of toughness reduction. In this regard, it would be worthwhile to consider $TiAl_3$ as the possible replacement for Co or Ni especially for the applications requiring a high hardness.

Vickers hardness indentations in the WC, and WC-10 vol.%$TiAl_3$ samples show typically one to three additional cracks propagating radially from the indentation as shown in Fig. 8. Fig. 9 shows a crack propagated in a deflective manner (↑) in WC-10 vol.%$TiAl_3$ composite. The enhanced fracture toughness of WC-10 vol.%$TiAl_3$ composite is believed that WC and $TiAl_3$ in the composite may deter the propagation of cracks and WC and $TiAl_3$ have nanostructure phases.

Conclusions

Using high frequency induction heated sintering (HFIHS), the rapid consolidation of the WC, and WC-10vol.%$TiAl_3$ was accomplished successfully. Nearly full-dense WC, and WC-10 vol.%$TiAl_3$ could be obtained within one min. The starting temperature of rapid densification and porosity of WC were reduced by the addition of $TiAl_3$. The average grain sizes of the WC are about 121 and 77 nm for the samples with WC, and WC-10 vol.%$TiAl_3$. The Vickers hardness and the fracture toughness values of the WC, and WC-10vol.%$TiAl_3$ samples were 2800 kg/mm^2, 6.2 MPa · m$^{1/2}$, and 2670 kg/mm^2, 9.5 MPa · m$^{1/2}$, respectively. The addition of $TiAl_3$ to WC improved the fracture toughness of cemented WC without great reduction of hardness. It would be worthwhile to consider $TiAl_3$ as the possible replacement for Co or Ni especially for the applications requiring a high hardness.

Acknowledgments

This research was supported by Basic Science Research Program though the National Research Foundation of Korea (NRF) funded by the Ministry of Education (2015R1D1A1A01056600) and this work was supported by the KIST Institutional Program (Project No. 2E25374-15-096).

References

1. S. Imasato, K. Tokumoto, T. Kitada, and S. Sakaguchi, Int. J. Refract. Met. Hard Mater. 13[5] (1995) 305-312.
2. G. Gille, J. Bredthauer, B. Gries, and B. Mende, Int. J. Refract. Met. Hard Mater. 18[2-3] (2000) 87-102.
3. P. Goeuriot, and F. Thevenot, Ceramics International 13[2] (1987) 99-103.
4. Z.G. Zhang, F. Gesmundo, and P.Y. Hou, and Y. Niu, Corrosion Science 48 (2006) 741-765.
5. H. Gleiter, Progress in Materials Science 33[4] (1989) 223-315.
6. G.E. Fougere, J.R. Weertman, R.W. Siegel, and S. Kim, Scripta Metallurgica et Materialia 26[12] (1992) 1879-1883.
7. Yaojun Lin, Wenchang Liu, Limin Wang, Enrique J. Lavernia, Materials Science & Engineering A573 (2013)197-204.
8. S. Berger, R. Porat, and R. Rosen, Prog. Mater. Sci. 42 (1997) 311-320.
9. B.R. Kang, and I.J. Shon, Korean J. Met. Mater. 53 (2015) 225-260.
10. I.J. Shon, H.G. Jo, and H.J. Kwon, Korean J. Met. Mater. 52 (2014) 343-346.
11. F. Charlot, E. Gaffet, B. Zeghmati, F. Bernard, and J.C. Niepce, Mater. Sci. Eng. A262 (1999) 279-278.
12. I.J. Shon, Korean J. Met. Mater. 52 (2014) 573-580.
13. M.K. Beyer, and H. Clausen-Schaumann, Chem. Rev. 105 (2005) 2921-2948.
14. J. Jung, and S. Kang, Scripta Materialia 56 (2007) 561-564.
15. H.S. Kang, J.M. Doh, J.K. Yoon, and I.J. Shon, Korean J. Met. Mater. 52 (2014) 759-764.
16. I.J. Shon, H.J. Kwon, and H.S. Oh, Korean J. Met. Mater. 52 (2014) 337-343.
17. H.S. Kang, S.L. Du, J.M. Doh, J.K. Yoon, and I.J. Shon, Electron. Mater. Lett. 10[3] (2014) 529-533.
18. H.G. Jo, and I.J. Shon, Journal of Ceramic Processing Research 15[6] (2014) 371-375.
19. C. Suryanarayana, M. Grant Norton, X-ray Diffraction: A Practical Approach, Plenum Press, New York, 1998.
20. G.S. Upadhyaya, Materials & Design 22[6] (2001) 483-489.
21. K. Niihara, R. Morena, and D.P.H. Hasselman, J. Mater. Sci. Lett. 1 (1982) 12-16.
22. I.J. Shon, I.K. Jeong, I.Y. Ko, J.M. doh, and K.D. Woo, Ceramics International 35 (2009) 339-344.